Express Polymer Letters Vol.16, No.2 (2022) 116–129
Available online at www.expresspolymlett.com
https://doi.org/10.3144/expresspolymlett.2022.10

Research article

Ionic cross-linked methacrylic copolymers for carbon fiber reinforced thermoplastic composites

Shiho Kuwashiro[1,2], *Nozomu Nakao*[2], *Satoshi Matsuda*[2], *Takeshi Kakibe*[2], *Hajime Kishi*[2*]

[1]Osaka Research Institute of Science and Technology Morinomiya Center, 1-6-50 Morinomiya, Joto-ku, Osaka-city, 536-8553 Osaka, Japan
[2]Graduate School of Engineering, University of Hyogo, 2167 Shosha, Himeji, 671-2201 Hyogo, Japan

Received 8 July 2021; accepted in revised form 17 September 2021

Abstract. Methacrylic copolymers have high potential as matrix polymers for carbon fiber reinforced thermoplastics (CFRTPs) due to their superior mechanical properties and the versatility of the monomers. However, the methacrylic copolymers have low solvent resistance, compared to epoxy, polyamide, and polypropylene, due to their un-cross-linked amorphous structure. Therefore, an improvement of the solvent resistance by the introduction of metal salts into methacrylic copolymer matrices for CFRTPs was investigated. Infrared spectroscopy, dynamic mechanical analyses and small-angle X-ray scattering clarified that an ionic cross-linked structure was formed. Low-viscosity mixtures of the methacrylic monomers with the metal salts, as a precursor of the matrices for CFRTPs, were easily impregnated into CF fabrics and were then copolymerized within the CF fabrics. Both the flexural strength and shear adhesive strength of the CFRTPs using the *in situ* polymerized methacrylic ionomer cross-linked with sodium ions were sufficiently high, even after 12 h immersion in methyl ethyl ketone.

Keywords: *polymer composites, ionomers, mechanical properties, thermal properties, solvent resistance*

1. Introduction

Carbon fiber reinforced thermoplastics (CFRTPs) are advanced lightweight materials that have been developed due to their high strength and high elastic modulus, with the potential for low-cost manufacturing and remolding ability. Several types of thermoplastic polymers, such as polyamide (PA) [1–7], polypropylene (PP) [8–10], polycarbonate (PC) [11, 12], polyether ether ketone (PEEK) [13–17], and polyphenylene sulfide (PPS) [18–20], have been studied for use as the matrices of CFRTPs.

Various methods have been researched for the fabrication of CFRTPs to achieve good impregnation of the thermoplastic polymer into the carbon fiber bundles. For continuous fiber filaments, the film stacking method [21, 22, 26], powder impregnation method [22–24, 26], and microblade method [25, 26] have been developed. However, the high viscosity of the polymers in any of the fabrication methods often prevents impregnation, which influences the mechanical properties of the resultant CFRTPs. Therefore, researchers have investigated suitable materials and molding conditions, such as pressure, temperature, and molding time, for the manufacture of high-quality CFRTPs [21–28]. Li *et al*. [23] reported two types of PEEKs with different melt flow rates; the polymer viscosity influenced the fiber distribution and mechanical properties. The low-viscosity polymer generated a better distribution of fibers in the CFRTP than the high-viscosity polymer, and the tensile strength of the CFRTP with low-viscosity polymer was 10–20% higher than that of CFRTP with the high-viscosity polymer [23].

Various monomer impregnation methods have been researched. For example, monomers (or oligomers) with low molecular weights are easily impregnated

*Corresponding author, e-mail: kishi@eng.u-hyogo.ac.jp

among fiber filaments due to their low viscosity. Parton and Verpoest [27] reported glass fiber reinforced thermoplastic polymers (GFRTP), where a precursor of polybutylene terephthalate, cyclic butylene terephthalate, was used. The low-viscosity oligomer was impregnated among GF bundles and was then polymerized. *in situ* polymerization of a polyamide 6 precursor, ε-caprolactam, was also reported for both CFRTP and GFRTP, in which good impregnation was achieved [28].

In our previous paper, methacrylic monomers were impregnated into plain woven CF fabrics and *in situ* bulk polymerization was conducted [29]. The improved interfacial adhesion using functional methacrylic copolymers imparted high flexural strength to the methacrylic CFRTP. The improved flexural strength of the methacrylic CFRTPs was almost equivalent to that of epoxy CFRPs.

However, methacrylic copolymers exhibit low solvent resistance, compared to epoxy, PA, and PP, because the methacrylic copolymer does not have a cross-linked or crystalline structure. The covalent cross-linking of polymers is effective to improve the solvent resistance; however, the characteristics of the thermoplastic polymer, such as the remolding ability, would be lost.

Therefore, improvement in the solvent resistance by the introduction of an ionic crosslinked structure into methacrylic copolymer matrices was investigated in this study. Although ionic cross-linked polymers, *i.e.*, ionomers, behave similarly to covalent cross-linked polymers at room temperature, they can deform and flow at high temperature [30]. Many researchers have reported the physical properties and structures of polymeric ionomers [30–34]. Ionomers with high toughness and abrasion resistance have been utilized for packaging materials, the outer skin of golf balls, ski boots, and automotive parts. Longworth and Vaughan [31] reported the physical structures of ionomers using X-ray diffraction and dynamic mechanical analysis, and the presence of ionic clusters in the ionomers was confirmed. The size of the ionic clusters as the high-order structure was *ca.* 10 nm in diameter and those ionic clusters were connected via the polymer chains. Eisenberg *et al*. [32] reported a new multiplet-cluster model for ionomers, where they insisted that the multiplet-clusters acted as cross-linking points that connected the polymer chains. Bonotto and Bonner [33] evaluated the ionomers using dynamic mechanical analyses; a rubbery plateau appeared when ethylene-acrylic acid copolymers were neutralized in the case of monovalent or divalent metal salts, and the rubbery plateau increased with the degree of neutralization. They reported that the phenomenon was similar to the increase in the cross-linking density of elastomers. The interaction of ionomers at the cross-link points decreased with an increase in temperature, which indicated that the ionomers would flow at high temperature. However, ionomers generally have a higher melt viscosity than the corresponding precursors without ionic cross-linking [30, 34]. Hirasawa *et al*. [34] showed that the melt viscosity of the polymer increased with ionomerization, *i.e.*, the degree of neutralization of the acrylic acid unit in the ethylene-acrylic acid copolymers.

There have been many reports on composite materials using ionomer matrices [35–43]. However, most of them were prepared by kneading short fibers or spherical fillers into the ionomer matrices. The fiber volume content (V_f) of short fiber composites is generally as low as 10–30 vol% [36, 37, 44, 45]. On the other hand, V_f can be set to 40 vol% or more in composites when the continuous fibers are oriented, which is advantageous for achieving high strength and high elastic modulus.

Tanaka *et al*. [46] examined the effect of the impregnation method on the mechanical properties of composites with short glass fibers or polyethylene fiber woven fabrics and glass ionomer cement matrices. It was reported that a pre-impregnation treatment was required to have sufficient flexural strength in the case of a polyethylene fiber woven fabric composites. Sundaresan *et al*. [47] reported on the self-healing properties of CFRTP in which continuous CF fibers were embedded in an ethylene-based ionomer film. However, there was no mention of the impregnation of the ionomers into the fiber bundles, and of the V_f for the composites. Sessini *et al*. [48] obtained composites with a sandwiched structure by compression molding using electrospinning microfibers because the ionomer matrix had high viscosity and it was difficult to impregnate into typical continuous fibers. However, the degree of alignment of the continuous fibers was low. In contrast, CFRP, in which the ionomers were used as interleaf films and laminated between layers of continuous fiber pre-impregnated materials (prepregs) has been studied for a long time, although the ionomers were not used as the matrix resin for the entire CFRP [41–43].

Therefore, to the best of our knowledge, there have been no reports on high V_f (>40 vol% CF) and high strength CFRTP composites using continuous CF fabrics and acrylic ionomer matrices, and research on achieving this is important. The main objective of this study was to create high V_f CFRTPs using continuous CF fabrics and methacrylic ionomer matrices with high solvent resistance. For this purpose, a fabrication method is proposed in which low-viscosity mixtures of methacrylic monomers with metal salts are impregnated into CF fabrics, instead of conventional highly viscous polymeric ionomers, and are copolymerized within the fabrics. The methacrylic ionomer CFRTPs fabricated via *in situ* polymerization were evaluated in terms of their mechanical properties, thermal resistance, solvent resistance, impregnation of the monomers, and the structure and properties of the ionomer matrices.

2. Experimental procedure

2.1. Materials

Two methacrylic monomers, methyl methacrylate (MMA; Sigma-Aldrich Japan) and methacrylic acid (MAA; Sigma-Aldrich Japan), were applied as raw materials to produce copolymers. 2,2′-Azobis(4-methoxy-2,4-dimethylvaleronitrile) (AMDVN; Wako Pure Chemical Industries, Ltd., Japan) was used as the polymerization initiator. The chemical structures of the monomers are shown in Figure 1. Sodium (Na) acetate and magnesium (Mg) acetate (Wako Pure Chemical Industries, Ltd., Japan) were utilized as the metal salts to form ionic cross-linked structures in the copolymers. Several metallic acetates, such as Na acetate, Mg acetate, lithium (Li) acetate, potassium (K) acetate, calcium (Ca) acetate, zinc (Zn) acetate, and aluminum (Al) acetate, were employed in preliminary experiments; however, only Na acetate, Mg acetate, Li acetate, and K acetate were dissolved in the methacrylic monomers. In this paper, Na^+ and Mg^{2+} were selected as representative monovalent and divalent ions.

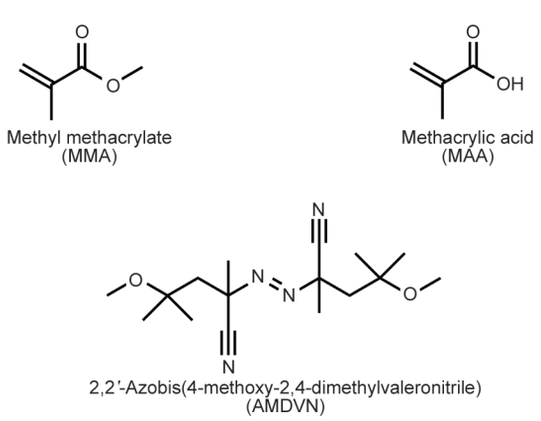

Figure 1. Chemical structures of the methacrylic monomers and initiator.

CF plain-woven fabric (CO6343B), which consists of T300B-3K (Toray Industries, Inc., Japan), was utilized as the reinforcement fibers for the acrylic CFRTPs. The areal density of the carbon fabric was 198 g/m^2.

2.2. Preparation of molded plates of methacrylic copolymers with metal salts

Molded plates of copolymers were prepared via bulk polymerization using a previously reported method [29]. Briefly, after removal of the polymerization inhibitors from the methacrylic monomers, monomers with 0.57 phm (parts per hundred of monomer) ADVN, and with or without Na acetate or Mg acetate metal salts were mixed using an ultrasonic generator. The molar ratio of the methacrylic monomers was MMA:MAA = 70:30. The mixtures were poured into Teflon-coated aluminum molds. The mixtures were copolymerized at 60 °C for 1 h in an oven, and then heated at 100 °C for 5 h and at 150 °C for 4 h. The second heating step was used to volatilize the trace amounts of acetic acid produced in the ion exchange reaction between the metallic acetate and the methacrylic acid. The size of the fabricated copolymer plate was 80×60×0.7 mm.

2.3. Fabrication of CFRPs

The mixtures of methacrylic monomers and initiators were prepared using the same procedure described in Section 2.2. The plain-woven CF fabric was placed in an aluminum mold, and an appropriately weighed amount of the methacrylic monomer mixture was poured into the mold. The monomers were then copolymerized in the CF fabrics at 60 °C for 2 h to obtain a prepreg sheet. The polymerized prepreg sheet (70×50 mm) was sandwiched between aluminum plates, and was then placed in an oven at 100 °C for 5 h and 150 °C for 4 h to produce a flat surface. Two prepregs were then stacked to fabricate specimens for lap-shear adhesion evaluation. Five prepregs were also stacked for flexural evaluation. The CFRTP laminates were fabricated from the stacked prepregs using a hot-pressing machine at 240 °C for 15 min under a pressure of 6 MPa. The CFRTPs with aluminum plates were then moved to

a cold-pressing machine to cool down to ambient temperature. The nominal V_f of the CFRTP laminates was controlled to 45 vol%. V_f was calculated using Equation (1), in which the density of the CFRTP (ρ) was measured using the Archimedes method. The densities of the polymer (ρ_m) and the fiber (ρ_f) were 1.20 and 1.80 g/cm^3, respectively:

$$V_f = \frac{\rho - \rho_m}{\rho_f - \rho_m} \quad (1)$$

2.4. Instrumental analyses of materials

2.4.1. Fourier transform infrared spectroscopy (FT-IR)

Fourier transform infrared (FT-IR) absorption spectra of polymers were measured with a spectrometer (FTIR 4100, JASCO, Japan) using the attenuated total reflectance (ATR) method with a diamond prism.

2.4.2. Dynamic mechanical analyses (DMA)

The temperature dependencies of the viscoelastic properties (storage modulus (E'), loss modulus (E''), and loss tangent (tan δ)) of the polymers were evaluated by dynamic mechanical analysis (DMA; DMS6100, Seiko Instruments, Japan) in tensile mode at an amplitude of 10 μm. A shear strain-controlled dynamic viscoelastometer (Rheosol-G5000NTD, UBM, Japan) with parallel plates (10 mm diameter with a gap of 700 μm) was used to evaluate the viscoelastic properties of the polymers in shear mode. Both tests were conducted at a dynamic frequency of 1 Hz, and a heating rate of 2 °C/min. The temperature range for tensile mode was from 20 to 180 °C, and that for shear mode was from 150 to 300 °C. The glass transition temperature (T_g) was defined as the peak temperature of the loss tangent (tan δ) in tensile mode. The rubbery plateau values of the storage modulus (G_r') were determined from the data in shear mode, and the molecular weight between cross-links (M_c) values were calculated based on rubber elasticity theory [49] using Equation (2) [50], where φ is a front factor (equivalent to the ratio of the mean square end-to-end distance of a network chain to that of a randomly coiled chain and assumed to equal 1.0 [51–53]), ρ is the density of the polymer (1.20 g/cm^3), R is the gas constant (8.31 J/(mol·K)), T_r is determined as T_g + 40 °C, and G_r' is the storage modulus in the rubbery plateau at T_g + 40 °C.

$$M_c = \frac{\varphi \rho R T_r}{G_r'} \quad (2)$$

2.4.3. Small-angle X-ray scattering (SAXS) analyses

SAXS analyses (D8 Discover Hybrid, BRUKER, Germany) were performed using Cu Kα radiation to detect the difference in the electron densities of the polymers. The scattering vector (q) is represented as Equation (3):

$$q = \frac{4\pi}{\lambda} \sin\Theta \quad (3)$$

where Θ is the diffraction angle and λ is the wavelength of the radiation (0.154 nm).

The SAXS curves can be analyzed using the Guinier approximation [54] (Equation (4)):

$$I(q) \sim \exp^{\frac{-q^2 R_g^2}{3}} \quad (4)$$

where $I(q)$ is the diffracted intensity and R_g is the radius of gyration. For spherical particles, the geometrical radius (R) is given using Equation (5):

$$R = \left(\frac{5}{3}\right)^{\frac{1}{2}} R_g \quad (5)$$

2.4.4. X-ray photoelectron spectroscopy (XPS)

X-ray photoelectron spectroscopy (XPS; PHI5000 VersaProbe, Ulvac-phi, inc., Japan) on the surface of CFs was performed with an Al Kα X-ray anode *in vacuo* at *ca.* $1 \cdot 10^{-6}$ Pa. The electron kinetic energy (*KE*) was calibrated using the highest *KE* component of the C_{ls} photoelectron peak for each sample as an internal reference. Relative sensitivity factors determined from the standard samples were used to estimate atomic ratios from peak area ratios.

2.5. Mechanical properties of polymers and CFRTPs

The mechanical properties of the polymers were evaluated using the flexural test mode. Specimens of polymers with a length of 40 mm, a width (b) of 10 mm, and a thickness (h) of 0.7 mm were machined from 0.7 mm thick polymer plates. Flexural stress-strain curves for several methacrylic copolymers were evaluated with a three-point bending configuration at a

cross-head speed of 2 mm/min and 23 °C using a mechanical testing machine (AUTOGRAPH AGS-J, Shimadzu, Japan). The elastic moduli (E) were calculated using Equation (6), in which k represents the initial slope of the load-displacement curve. The span length (L) for the three-point bending was 20 mm:

$$E = \frac{L^3}{4bh^3}k \tag{6}$$

To examine the interfacial adhesion between the CFs and the matrix polymers, the shear adhesive strengths of the CFRTPs were evaluated in the lap-shear configuration under a tensile strain rate of 2 mm/min at 23 °C using a mechanical testing machine (AUTOGRAPH AGS-J, Shimadzu, Japan). The lap area had a length of 6 mm and a width of 6 mm. The testing method followed the JIS K 6850:1999 standard.

The flexural strength of the CFRTP laminates was measured using a four-point bending configuration with a cross-head speed of 2 mm/min at 23 °C, using a mechanical testing machine (AUTOGRAPH AGS-J, Shimadzu, Japan). The specimen length was 60 mm, the width (b) was 10 mm, the thickness (h) was 1.2 mm, and the span length (L) for the four-point bending was 30 mm. The elastic moduli (E) and flexural strengths (σ_B) were calculated using Equations (7) and (8), in which P_{max} is the maximum force and k represents the initial slope of the load-displacement curve. The testing method followed the JIS K 7074:1988 standard:

$$E = \frac{23L^3}{108bh^3}k \tag{7}$$

$$\sigma_B = \frac{P_{max}L}{bh^2} \tag{8}$$

The polymers and CFRTP laminates were pre-soaked in methyl ethyl ketone (MEK) at 23 °C for 12 h, and the mechanical properties were evaluated to examine the solvent resistance.

2.6. Microscopic observation

Cross-sections of the CFRTP laminates were observed using optical microscopy (OM; BX50, Olympus, Japan) in reflecting light mode. The specimens were cut using a diamond saw, and the sides were polished petrographically prior to observations. The fracture surfaces of the CFRTP laminates were observed using scanning electron microscopy (SEM; VE-9800, Keyence, Japan). The samples were mounted on brass stubs and coated with a thin layer of platinum using an ion sputter coater (JFC1100E, JEOL, Japan).

3. Results and discussion

3.1. Chemical structures of methacrylic copolymers containing metal salts

Mixtures of methacrylic monomers with metal salts (sodium or magnesium salts) were first polymerized. Figure 2 shows FT-IR spectra of the methacrylic copolymers and the metal salt blends. The absorbances at 1140 and 1720 cm^{-1} correspond to C–O and C=O, respectively, of the ester structure in poly (methyl methacrylate) (PMMA). A shoulder at 1696 cm^{-1} appeared by copolymerization with MAA, which corresponded to –COOH groups in the methacrylic acid units. After blending with sodium acetate, the methacrylic copolymer showed a new absorbance at 1550 cm^{-1}. In the case of blending magnesium acetate, two absorbance shoulders appeared at 1550 and 1630 cm^{-1}, and the shoulder at 1696 cm^{-1} became unclear. The absorbance bands at 1550 and 1630 cm^{-1} correspond to COO^-, which indicated ionic bonds were formed in the methacrylic copolymer by ion exchange reaction between –COOH groups and the metal salts [55–57]. According to Han and Williams [57], the new absorbance peaks in the region at 1480–1670 cm^{-1} corresponded to COO^- for poly(ethylene-*co*-methacrylic) ionomers. The new absorbance peaks were reported to increase with the amount of metal salts, and the absorbance at 1696 cm^{-1} corresponding to –COOH groups decreased. The new absorbance for the ionomer with

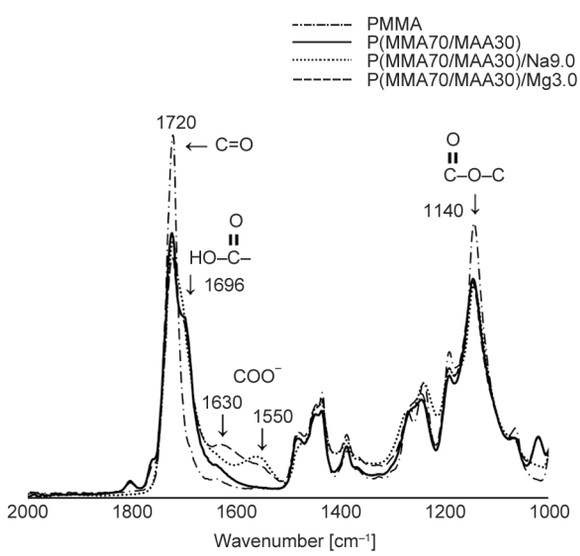

Figure 2. FT-IR spectra for methacrylic copolymers and ionomers.

Mg^{2+} was reported to appear at higher wavenumber than that for the ionomer with Na^{+}. Figure 2 shows the results are consistent with those reported by Han and Williams [57].

3.2. Physical structures of methacrylic copolymers containing metal salts

Table 1 summarizes the viscoelastic properties of the methacrylic copolymers obtained from dynamic mechanical analyses in both tensile mode and shear mode. The glass transition temperatures (T_gs) were measured in tensile mode and the rubbery plateau was measured in shear mode. Relaxation of the storage modulus around the T_g of the methacrylic copolymers containing sodium salts became gradual, and the full width at half maximum (FWHM) of the tan δ peak corresponding to T_g became wider than that of the original methacrylic copolymers without metal salts. The FWHM of the tan δ peak became wider as the amount of the sodium salts increased. Similar results were also obtained for the methacrylic copolymers containing magnesium salts. The FWHM of the tan δ peak was wider than that of the methacrylic copolymers containing sodium salts. These results indicated that the addition of metal salts caused the distribution of molecular mobility in the methacrylic copolymer, which was dependent on the content and types of metal salt. Eisenberg *et al*. [32] clarified that the increase in the width of the loss tangent peak reflected restriction of the mobility of the polymer chains with multiplets. Kishi *et al*. [58] explained the FWHM represented the heterogeneity of the cross-link density of the networked polymers.

Figure 3 shows the storage moduli around the rubbery plateau region (G_r') of the methacrylic copolymers and ionomers. The flow temperature of the original methacrylic copolymer, P(MMA70/MAA30), was around 240 °C, whereas the methacrylic copolymers containing 3 mol% sodium salts, P(MMA70/MAA30)/Na3.0, showed a long rubbery plateau and flowed at 280 °C (Figure 3a).

The methacrylic copolymer with 9 mol% sodium salt, P(MMA70/MAA30)/Na9.0, had a higher G_r' than the copolymer with 3 mol% sodium salt, P(MMA70/MAA30)/Na3.0. The extension of the rubbery plateau region and the change in G_r' with the metal salt content indicated the formation of an ionic cross-linked structure in the polymer chains [33]; the increase in G_r' indicated an increase in the ionic cross-linked points. The M_c of these polymers was calculated using Equation (1) and is given in Table 1. The M_c decreased with an increase in the sodium salt content, *i.e.*, the cross-link density increased. No flow point was detected in the case of copolymer modified

Table 1. Dynamic mechanical analyses of the methacrylic copolymers and ionomers.

Copolymerization ratio [mol%] Ion content [mol%]	Tensile mode		Shear mode	
	T_g [°C]	FWHM of tan δ peak at T_g [°C]	Rubbery plateau, G_r' [MPa]	Molecular weight between cross-linked points, M_c [mol/g]
P(MMA70/MAA30)	150	28	0.59	7825*
P(MMA70/MAA30)/Na3.0	157	38	0.65	7211
P(MMA70/MAA30)/Na9.0	173	66	0.95	5101
P(MMA70/MAA30)/Mg3.0	153	109	0.91	5107

*The molecular weight between entanglements (M_e)

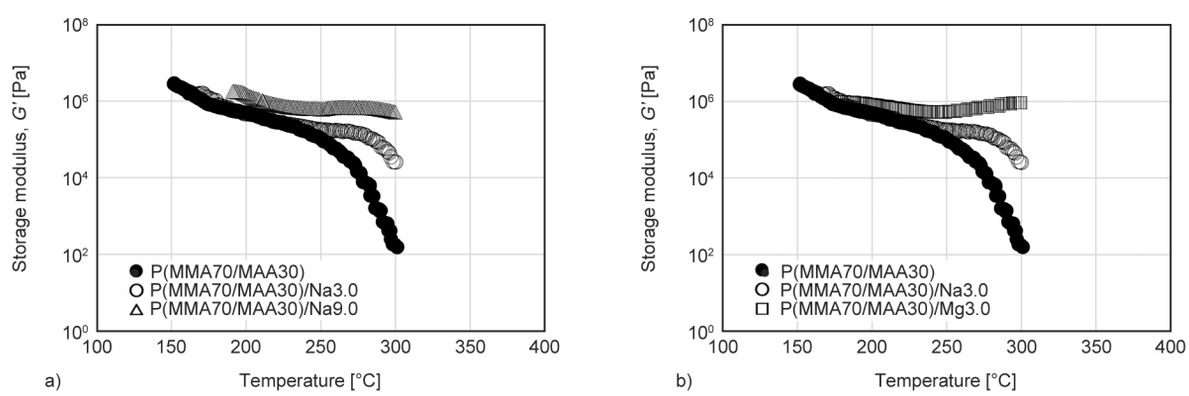

Figure 3. Temperature dependence of storage modulus G' of methacrylic copolymers and ionomers. (a) Dependence of the storage modulus G' on the sodium salt content. (b) Dependence of the storage modulus G' on the type of metal salt.

with 3 mol% magnesium salt, P(MMA70/MAA30)/Mg3.0, in the measurement range (Figure 3b). Figure 3b shows that the magnesium salts had a stronger ionic bonding force than the sodium salt. Hara *et al*. [59] reported that the length of the rubbery plateau region of sulfonated polystyrene ionomers became longer for the divalent Ca ionomer than the monovalent K and Cs ionomers, *i.e.*, the strength of the ionic interactions was greater for divalent ions than for monovalent ions. Ionic cross-linking generally has a thermo-reversible nature, and the flow temperature could be controlled by selection of the type and content of the metal salt. The results suggest that the sodium ionomer has an advantage in terms of the thermoplastic properties when compared to the magnesium ionomer.

FT-IR and DMA data obtained in these studies have clarified that metal ionic cross-links are formed in blends consisting of *in situ* polymerized P(MMA/MAA) and metal salts. The internal structure was further investigated using SAXS. Figure 4a shows SAXS profiles of the methacrylic copolymer and the ionomers. No peaks to indicate the existence of periodical structures were evident in all polymers; however, there was difference in the SAXS intensity, especially in the small-angle region. The intensity in the low-q region of the methacrylic ionomer with 9 mol% Na and that with 3 mol% Mg were higher than that of the methacrylate copolymer. The results clearly indicate that a difference in electron density exists in the methacrylic ionomers.

The size of the region of electron density fluctuation can be calculated as the radius of gyration (R_g) using the Guinier approximation, shown as Equation (3) [54, 60]. From the slope of regression line in the low-q region in Figure 4b, the R_g values of the methacrylic ionomer with 9 mol% Na and that of the ionomer with 3 mol% Mg were calculated to be 5.98 and 7.57 nm, respectively. Assuming that the particles are spherical, the average radius R can be calculated using Equation (4) to be 7.72 and 9.77 nm, respectively. The sizes of R have approximate coincidence with the size of the ionic cluster (10 nm) reported by Longworth and Vaughan [31]. It was assumed that an ionic cluster may be formed in the polymers when the metal salts are dissolved in the methacrylic monomers, followed by polymerization while maintaining the ionic cluster.

3.3. Solvent resistance of methacrylic copolymers containing metal salts

One of the drawbacks of amorphous polymers is low solvent resistance. Here, polymerized specimens from mixtures of the methacrylic monomers with metal salts were prepared, and the change in the solvent resistance by ionic cross-linking was then evaluated. Figures 5a and 5b show elastic moduli of methacrylic copolymers with or without metal salts. Mg acetate had lower solubility in the methacrylic monomers than Na acetate. When Mg acetate was added at more than 3 mol%, a white precipitate was formed in the mixture. Therefore, the concentration of Mg was experimentally limited to 3 mol%. Figure 5b shows that PMMA and P(MMA/MAA) without metal salts were completely dissolved in MEK after immersion for 12 h; therefore, no elastic modulus was measurable. In contrast, the methacrylic copolymers containing metal salts were not dissolved in MEK, and the elastic moduli were 3 GPa or more both before and after immersion in MEK. Therefore, the addition of metal salts was effective to improve the solvent resistance of the methacrylic copolymers and

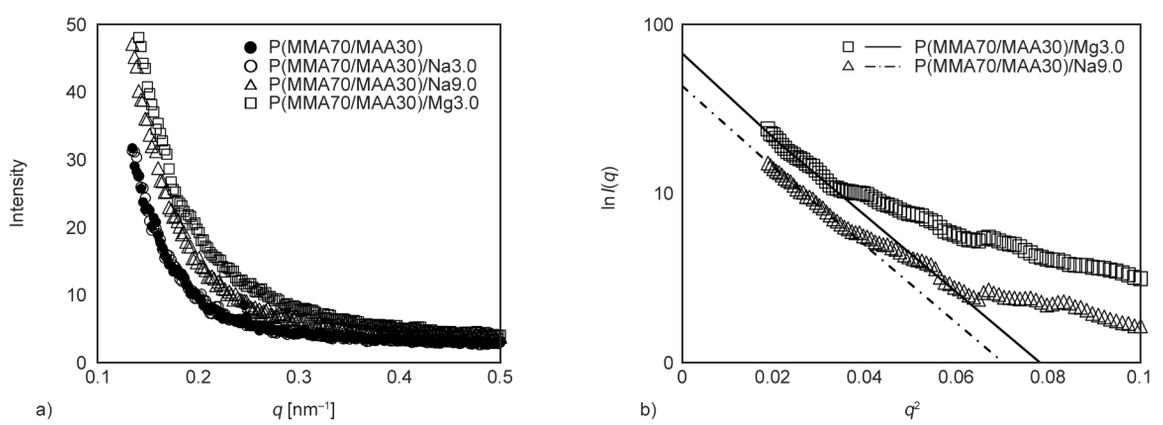

Figure 4. SAXS analyses of methacrylic copolymers and the ionomers. (a) SAXS profile of methacrylic copolymers and ionomers. (b) Guinier approximation from the SAXS profile.

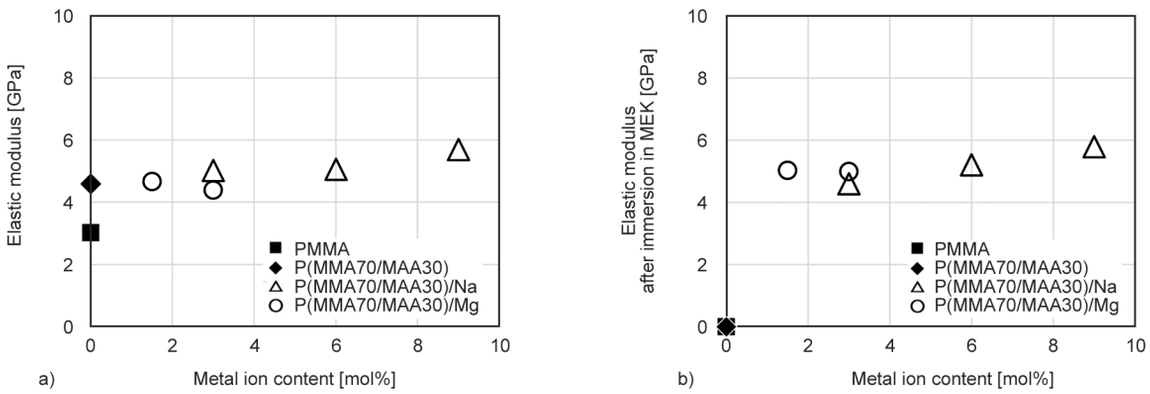

Figure 5. Relationship between elastic moduli of P(MMA/MAA) ionomers and the metal ion content. (a) Elastic moduli of P(MMA/MAA) copolymers and ionomers before immersion in MEK. (b) Elastic moduli of P(MMA/MAA) copolymers and ionomers after immersion in MEK for 12 h at 23 °C.

keep the high elastic moduli. The ionic cross-linked structure was the reason for the improved solvent resistance of the methacrylic copolymers. A matrix polymer with a high elastic modulus is an important requirement to achieve the high compressive strengths and high flexural strengths of CFRPs [61].

3.4. Mechanical properties of methacrylic ionomer CFRTPs and the solvent resistance

Methacrylic ionomer (ionic cross-linked methacrylic copolymer) matrix CFRTPs were fabricated via the impregnation of monomers including metal salts into CF fabrics and the *in situ* polymerization. The mixtures of both methacrylic monomers with 3 mol% Na salt and monomers with 3 mol% Mg salt had low viscosity, so that they were easily impregnated into the CF fabrics. No noticeable voids were evident in ionomer CFRTP laminates with 3 mol% Na salt, CF/P(MMA70/MAA30)/Na3.0, as shown in Figure 6a, which demonstrates the advantage of using the monomer impregnation method for the fabrication of methacrylic ionomer CFRTPs. However, the CFRTP laminates with 3 mol% Mg salt, CF/P(MMA70/MAA30)/Mg3.0, had large voids in the interlaminar region, as shown in Figure 6b.

Figure 7 shows the flexural strength, elastic modulus, and lap shear adhesive strength for the methacrylic CFRTP laminates. Figure 7a shows that the flexural strength of the methacrylic CFRTPs increased with increasing adhesive strength. The flexural strength and the lap shear adhesive strength for CF/P(MMA70/MAA30) and CF/P(MMA70/MAA30)/Na3.0 was higher than those for CF/PMMA and CF/P(MMA70/ MAA30)/Mg3.0. In particular, the CF/P(MMA70/ MAA30)/Mg3.0 laminates had poor

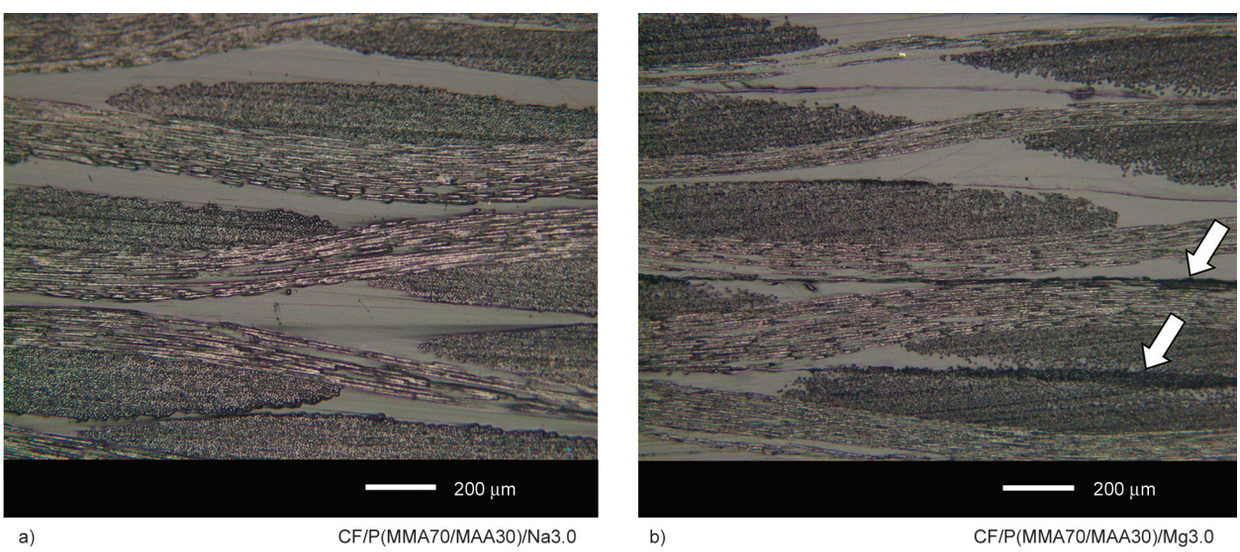

Figure 6. Cross sections of (a) CF/P(MMA70/MAA30)/Na3.0 and (b) CF/P(MMA70/MAA30)/Mg3.0 laminates. The white arrows in (b) indicate large voids in the interlaminar region.

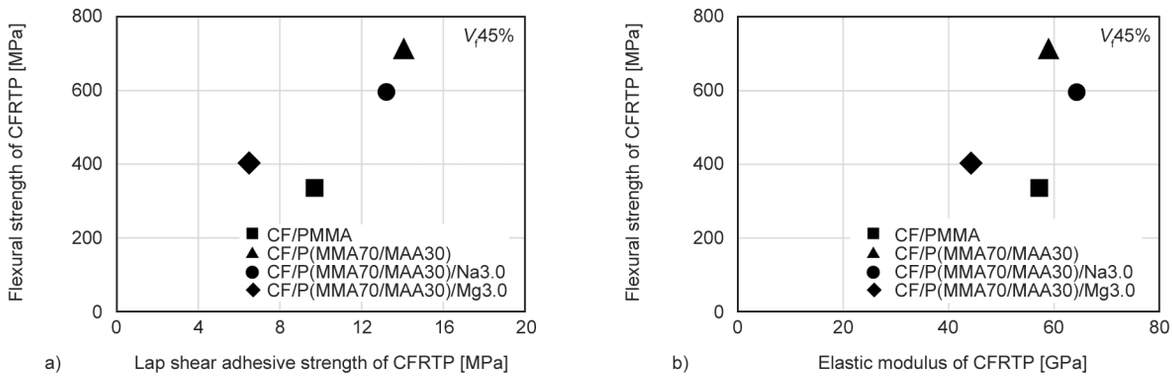

Figure 7. Mechanical properties of methacrylic CFRTPs. (a) Flexural strength and lap shear adhesive strength of CFRTPs. (b) Flexural strength and elastic modulus of CFRTPs.

adhesive and flexural properties. The CF/P(MMA70/MAA30)/ Mg3.0 laminates had a large number of voids in the interlaminar region. The CFRTP laminates were fabricated from stacked prepregs using a hot-pressing machine at 240 °C. At this temperature, the viscosity of the P(MMA70/MAA30)/Mg3.0 matrix was considerably higher than that for the P(MMA70/MAA30)/Na3.0 matrix, as shown in Figure 3b. The low flowability caused low adhesive strength between the prepregs, which led to buckling failure mode with delamination of the layers under the flexural load, *i.e.*, the laminates had a low flexural strength and elastic modulus, as shown in Figure 7b. These results indicate that the use of monovalent Na^+ ions offers advantages over divalent Mg^{2+} ions in terms of the total balance of properties required for the matrix polymer of the CFRTP laminates.

Figure 8 shows the fractured surfaces of CFRTP specimens after the flexural tests. The PMMA matrix polymer was peeled off from the CFs during the fracture process due to poor interfacial adhesive strength, and the surfaces of the CFs were exposed, as shown in Figure 8a. However, the P(MMA70/MAA30) copolymer matrix, the P(MMA70/MAA30)/Na3.0 ionomer matrix, and the P(MMA70/MAA30)/Mg3.0 ionomer matrix remained adhered to the CFs, as shown in Figures 8b–8d. Therefore, the copolymerization of MAA was very effective to improve the adhesive strength to the CFs.

X-ray photoelectron spectroscopy (XPS) analyses reported the presence of small amounts of functional groups on the surface of commercially available CFs [62–64]. XPS analyses were also conducted in this study on CF plain-woven fabric (CO6343B), which consists of T300B-3K, after removal of the sizing agents on the CFs by immersion in dimethyl sulfoxide (DMSO) and MEK. The O_{1s}/C_{1s} ratio was 0.22, which suggested the presence of the oxidized functional groups. The curve fitting for the spectra separation indicated the presence of hydroxyl groups and carboxyl groups on the surface of the CFs, as shown in Figure 9.

It was thus expected that positive interactions such as hydrogen bonding and dipole interactions between functional groups on the CFs and carboxyl groups of the matrix copolymers act to promote adhesion. In the case of the methacrylic ionomer, some carboxyl groups were neutralized by the metal salts. However, free carboxyl groups would remain because the ratio of neutralization was 10%. Therefore, high adhesive strength between the CFs and the matrix polymer was also maintained in the methacrylic ionomer matrix CFRTP.

Even after immersion in MEK for 12 h, the strength of the methacrylic ionomer CFRTP laminates with Na salts was considerable, as shown in Figure 10. On the other hand, both composites of PMMA matrix and P(MMA70/MAA30) matrix without Na salts were completely dissolved and both the flexural and adhesive strengths could not be measured. Here, compared to the decrease in the flexural strength, the decrease in the shear adhesive strength of the ionomer matrix CFRTP laminate with Na salt, CF/P(MMA70/MAA30)/Na3.0, was small with only a 10% decrease detected. Even after immersion in MEK, the ionomer matrix adhered well to the CFs, as shown in Figure 11. This suggests that deterioration of the interfacial adhesion during MEK immersion may not be the major reason for the decrease in flexural strength. The elastic modulus of the CFRTP decreased by approximately 36%; however, the elastic modulus of the polymer did not decrease, as shown in Figure 5. One plausible assumption with regard

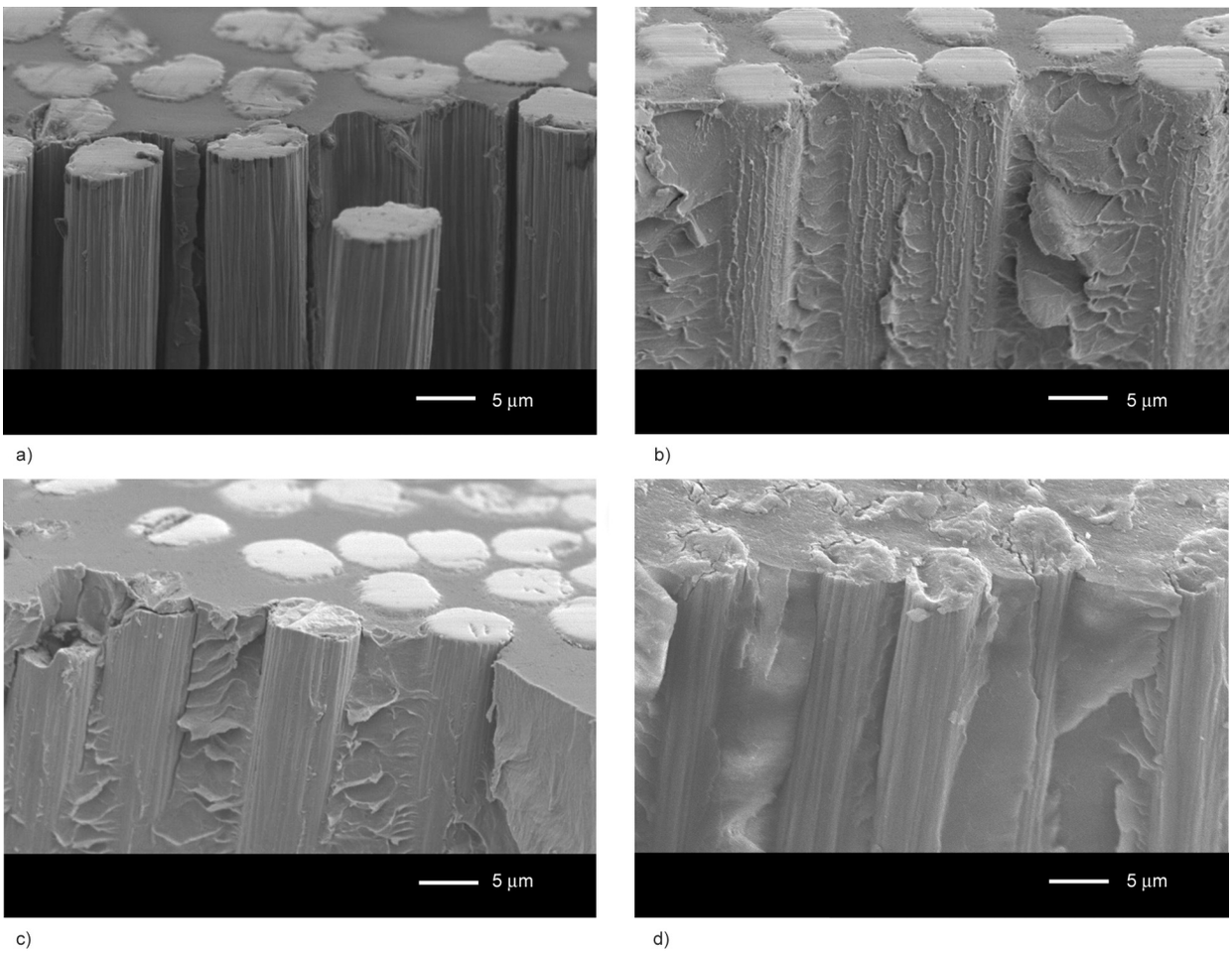

Figure 8. SEM micrographs of fracture surfaces of methacrylic CFRTPs. (a) CF/PMMA, (b) CF/P(MMA-MAA), (c) CF/P(MMA70/MAA30)/Na3.0, (d) CF/P(MMA70/MAA30)/Mg3.0.

to the decrease in the flexural strength of CFRTP would be local plasticization (decrease in the elastic modulus) of the ionomer matrix adjacent to the interface with CFs by the absorption of MEK.

4. Conclusions

Mixtures of methacrylic monomers (MMA and MAA) with Na or Mg salts were polymerized, and the structure and properties of the resultant methacrylic copolymers were investigated. FT-IR, DMA, and SAXS measurements clarified that an ionic cross-link structure was formed in the specimens consisting of the P(MMA/MAA) methacrylic copolymers and metal salts. The ionic cross-linked structure acted to increase the solvent resistance of the methacrylic copolymer. Low-viscosity mixtures of the methacrylic

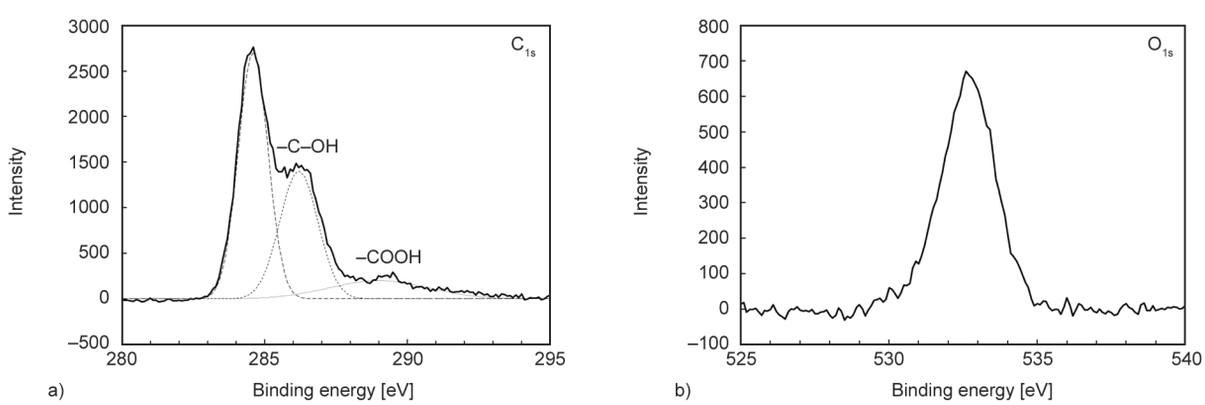

Figure 9. XPS spectrum of the surface of the CFs. (a) C_{1s}. (b) O_{1s}.

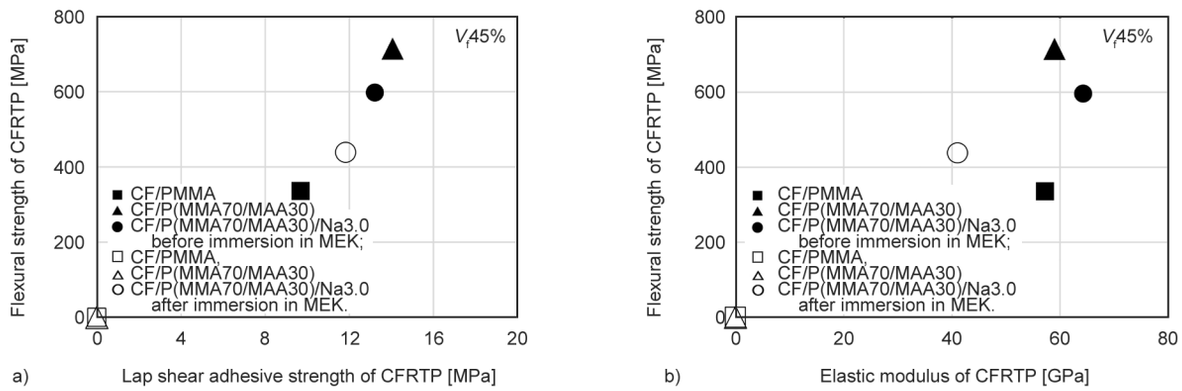

Figure 10. Mechanical properties of methacrylic CFRTPs before and after immersion in MEK. (a) Flexural strength and lap shear adhesive strength of CFRTP, before and after immersion in MEK. (b) Flexural strength and elastic modulus of CFRTP, before and after immersion in MEK.

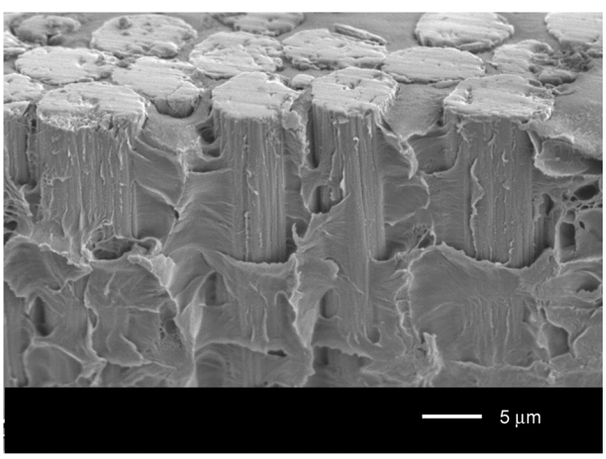

Figure 11. SEM micrographs of CF/P(MMA70/MAA30) Na3.0 fracture surface after immersion in MEK.

monomers with metal salts, as a precursor of the matrix polymer of the CFRTP, were easily impregnated into CF fabrics. For the methacrylic ionomer cross-linked with Na^+ ions, both the flexural and shear strengths of the *in situ* polymerized CFRTP laminates were sufficiently high, even after 12 h immersion in MEK. However, when Mg^{2+} ions were used, the strength of the CFRTP laminates was not sufficient, due to the low adhesion between the laminates caused by the high viscosity of the Mg^{2+} cross-linked ionomers. This study proposed a successful new process for the fabrication of thermoplastic methacrylic ionomer composites with high strength and high solvent resistance.

Acknowledgements

The authors would like to thank those at TORAY COATEX CO., LTD, especially Mr. Satoshi Ogasa and Mr. Kazuhiko Kominami, for preparation of some of the materials and for helpful discussions.

References

[1] Djumaev A., Takahashi K.: Effect of moisture absorption on damping performance and dynamic stiffness of NY-6/CF commingled yarn composite. Journal of Materials Science, **29**, 4736–4741 (1994). https://doi.org/10.1007/BF00356517

[2] Choi N. S., Yamaguchi H., Takahashi K.: Fracture behavior of unidirectional commingled-yarn-based carbon fiber/polyamide 6 composite under three-point bending. Journal of Composite Materials, **30**, 760–784 (1996). https://doi.org/10.1177/002199839603000701

[3] An H. J., Kim J. S., Kim K-Y., Lim D. Y., Kim D. H.: Mechanical and thermal properties of long carbon fiber-reinforced polyamide 6 composites. Fibers and Polymers, **15**, 2355–2359 (2014). https://doi.org/10.1007/s12221-014-2355-5

[4] Mohd Ishak Z. A., Berry J. P.: Hygrothermal aging studies of short carbon fiber reinforced nylon 6.6. Journal of Applied Polymer Science, **51**, 2145–2155 (1994). https://doi.org/10.1002/app.1994.070511306

[5] Karsli N. G., Ozkan C., Aytac A., Deniz V.: Effects of sizing materials on the properties of carbon fiber-reinforced polyamide 6,6 composites. Polymer Composites, **34**, 1583–1590 (2013). https://doi.org/10.1002/pc.22556

[6] Czigány T., Karger-Kocsis J.: A comparison of the mechanical behaviour of weft-knitted glass and carbon fiber fabric-reinforced polyamide-12 composites produced with commingled staple yarns. Polymers and Polymer Composites, **9**, 491–498 (2001). https://doi.org/10.1177/096739110100900801

[7] Czigány T., Mohd Ishak Z. A., Karger-Kocsis J.: On the failure mode in dry and hygrothermally aged short fiber-reinforced injection-molded polyarylamide composites by acoustic emission. Applied Composite Materials, **2**, 313–326 (1995). https://doi.org/10.1007/BF00568767

[8] Dean D. M., Marchione A. A., Rebenfeld L., Register R. A.: Flexural properties of fiber-reinforced polypropylene composites with and without a transcrystalline layer. Polymers for Advanced Technologies, **10**, 655–668 (1999). https://doi.org/10.1002/(SICI)1099-1581(199911)10:11<655::AID-PAT919>3.0.CO;2-%23

[9] Szentes A., Varga Cs., Horváth G., Bartha Z., Kónya Z., Haspel H., Szél J., Kukovecz A.: Electrical resistivity and thermal properties of compatibilized multi-walled carbon nanotube/polypropylene composites. Express Polymer Letters, **6**, 494–502 (2012). https://doi.org/10.3144/expresspolymlett.2012.52

[10] Arao Y., Yumitori S., Suzuki H., Tanaka T., Tanaka K., Katayama T.: Mechanical properties of injection-molded carbon fiber/polypropylene composites hybridized with nanofillers. Composites Part A: Applied Science and Manufacturing, **55**, 19–26 (2013). https://doi.org/10.1016/j.compositesa.2013.08.002

[11] Montes-Morán M. A., Martínez-Alonso A., Tascón J. M. D., Paiva M. C., Bernardo C. A.: Effects of plasma oxidation on the surface and interfacial properties of carbon fibres/polycarbonate composites. Carbon, **39**, 1057–1068 (2001). https://doi.org/10.1016/S0008-6223(00)00220-7

[12] Montes-Morán M. A., van Hattum F. W. J., Nunes J. P., Martínez-Alonso A., Tascón J. M. D., Bernardo C. A.: A study of the effect of plasma treatment on the interfacial properties of carbon fibre–thermoplastic composites. Carbon, **43**, 1795–1799 (2005). https://doi.org/10.1016/j.carbon.2005.02.005

[13] Tiwari S., Sharma M., Panier S., Mutel B., Mitschang P., Bijwe J.: Influence of cold remote nitrogen oxygen plasma treatment on carbon fabric and its composites with specialty polymers. Journal of Materials Science, **46**, 964–974 (2011). https://doi.org/10.1007/s10853-010-4847-z

[14] Seferis J. C.: Polyetheretherketone (PEEK): Processing-structure and properties studies for a matrix in high performance composites. Polymer Composites, **7**, 158–169 (1986). https://doi.org/10.1002/pc.750070305

[15] Velisaris C. N., Seferis J. C.: Crystallization kinetics of polyetheretherketone (PEEK) matrices. Polymer Engineering and Science, **26**, 1574–1581 (1986). https://doi.org/10.1002/pen.760262208

[16] Ostberg G. M. K., Seferis J. C.: Annealing effects on the crystallinity of polyetheretherketone (PEEK) and its carbon fiber composite. Journal of Applied Polymer Science, **33**, 29–39 (1987). https://doi.org/10.1002/app.1987.070330103

[17] Yoon H., Takahashi K.: Mode I interlaminar fracture toughness of commingled carbon fibre/PEEK composites. Journal of Materials Science, **28**, 1849–1855 (1993). https://doi.org/10.1007/BF00595757

[18] Sharma M., Bijwe J., Mitschang P.: Wear performance of PEEK–carbon fabric composites with strengthened fiber–matrix interface. Wear, **271**, 2261–2268 (2011). https://doi.org/10.1016/j.wear.2010.11.055

[19] Kenny J. M., Maffezzoli A.: Crystallization kinetics of poly(phenylene sulfide) (PPS) and PPS/carbon fiber composites. Polymer Engineering and Science, **31**, 607–614 (1991). https://doi.org/10.1002/pen.760310812

[20] Jiang Z., Gyurova L. A., Schlarb A. K., Friedrich K., Zhang Z.: Study on friction and wear behavior of polyphenylene sulfide composites reinforced by short carbon fibers and sub-micro TiO_2 particles. Composites Science and Technology, **68**, 734–742 (2008). https://doi.org/10.1016/j.compscitech.2007.09.022

[21] Cender T. A., Simacek P., Advani S. G.: Resin film impregnation in fabric prepregs with dual length scale permeability. Composites Part A: Applied Science and Manufacturing, **53**, 118–128 (2013). https://doi.org/10.1016/j.compositesa.2013.05.013

[22] Vaidya U. K., Chawla K. K.: Processing of fibre reinforced thermoplastic composites. International Materials Reviews, **53**, 185–218 (2008). https://doi.org/10.1179/174328008X325223

[23] Li X., Zhao Y., Wang K., Chen J., Lu W.: Study on the rheology and tensile property of CCF300/PEEK composites *via* powder impregnation. in 'Proceeding of 21st International Conference on Composite Materials. Xi'an, China' 4693 p4 (2017).

[24] Iyer S. R., Drzal L. T.: Manufacture of powder-impregnated thermoplastic composites. Journal of Thermoplastic Composite Materials, **7**, 325–355 (1990). https://doi.org/10.1177/089270579000300404

[25] Kobayashi S., Takada K.: Processing of unidirectional hemp fiber reinforced composites with micro-braiding technique. Composites Part A: Applied Science and Manufacturing, **46**, 173–179 (2013). https://doi.org/10.1016/j.compositesa.2012.11.012

[26] Kazano S., Osada T., Kobayashi S., Goto K.: Experimental and analytical investigation on resin impregnation behavior in continuous carbon fiber reinforced thermoplastic polyimide composites. Mechanics of Advanced Materials and Modern Processes, **4**, 6 (2018). https://doi.org/10.1186/s40759-018-0039-3

[27] Parton H., Verpoest I.: *In situ* polymerization of thermoplastic composites based on cyclic oligomers. Polymer Composites, **26**, 60–65 (2005). https://doi.org/10.1002/pc.20074

[28] Ben G., Hirabayashi A., Sakata K., Nakamura K., Hirayama N.: Evaluation of new GFRTP and CFRTP using epsilon caprolactam as matrix fabricated with VaRTM. Science and Engineering of Composite Materials, **22**, 633–641 (2015). https://doi.org/10.1515/secm-2014-0013

[29] Kishi H., Nakao N., Kuwashiro S., Matsuda S.: Carbon fiber reinforced thermoplastic composites from acrylic polymer matrices: Interfacial adhesion and physical properties. Express Polymer Letters, **11**, 334–342 (2017). https://doi.org/10.3144/expresspolymlett.2017.32

[30] Fujiyama M., Kondou M., Ayama K., Inata H.: Rheological properties of ionically and covalently cross-linked polypropylene-type thermoplastic elastomers. Journal of Applied Polymer Science, **85**, 762–773 (2002). https://doi.org/10.1002/app.10644

[31] Longworth R., Vaughan D. J.: Physical structure of ionomers. Nature, **218**, 85–87 (1968). https://doi.org/10.1038/218085a0

[32] Eisenberg A., Hird B., Moore R. B.: A new multiplet-cluster model for the morphology of random ionomers. Macromolecules, **23**, 4098–4107 (1990). https://doi.org/10.1021/ma00220a012

[33] Bonotto S., Bonner E. F.: Effect of ion valency on the bulk physical properties of salts of ethylene-acrylic acid copolymers. Macromolecules, **1**, 510–515 (1968). https://doi.org/10.1021/ma60006a011

[34] Hirasawa E., Yamamoto Y., Tadano K., Yano S.: Effect of metal cation type on the structure and properties of ethylene ionomers. Journal of Applied Polymer Science, **42**, 351–362 (1991). https://doi.org/10.1002/app.1991.070420207

[35] Alesi A. L., Litman A. M., Mitchell D. F.: Aramid fiber-reinforced ionomer. Polymer Engineering and Science, **18**, 1209–1215 (1978). https://doi.org/10.1002/pen.760181604

[36] Papaspyrides C. D., Poulakis J. G., Arvanitopoulos C. D.: Recycling of glass fiber reinforced thermo-plastic composites. I. Ionomer and low density polyethylene based composites. Resources, Conservation and Recycling, **14**, 91–101 (1995). https://doi.org/10.1016/S0921-3449(95)80003-4

[37] Takayanagi M., Kajiyama T., Katayose T.: Surface-modified kevlar fiber-reinforced polyethylene and ionomer. Journal of Applied Polymer Science, **27**, 3903–3917 (1982). https://doi.org/10.1002/app.1982.070271024

[38] Post W., Bose R. K., Garcia S. J., van der Zwaag S.: Healing of early stage fatigue damage in ionomer/Fe_3O_4 nanoparticle composites. Polymers, **8**, 436 (2016). https://doi.org/10.3390/polym8120436

[39] Sessini V., Brox D., López A. J., Ureña A., Peponi L.: Thermally activated shape memory behavior of copolymers based on ethylene reinforced with silica nanoparticles. Nanocomposites, **4**, 19–35 (2018). https://doi.org/10.1080/20550324.2018.1472723

[40] Hammouda I. M.: Reinforcement of conventional glass-ionomer restorative material with short glass fibers. Journal of the Mechanical Behavior of Biomedical Materials, **2**, 73–81 (2009). https://doi.org/10.1016/j.jmbbm.2008.04.002

[41] Kishi H., Kuwata M., Matsuda S., Asami T., Murakami A.: Damping properties of thermoplastic-elastomer interleaved carbon fiber-reinforced epoxy composites. Composites Science and Technology, **64**, 2517–2523 (2004). https://doi.org/10.1016/j.compscitech.2004.05.006

[42] Kim J. W., Lee J. S.: Influence of interleaved films on the mechanical properties of carbon fiber fabric/polypropylene thermoplastic composites. Materials, **9**, 344 (2016). https://doi.org/10.3390/ma9050344

[43] Matsuda S., Hojo M., Ochiai S., Murakami A., Akimoto H., Ando M.: Effect of ionomer thickness on mode I interlaminar fracture toughness for ionomer toughened CFRP. Composites Part A: Applied Science and Manufacturing, **30**, 1311–1319 (1999). https://doi.org/10.1016/S1359-835X(99)00023-8

[44] Okada M., Kato T., Otsu M., Tanaka H., Miura T.: Development of optical-heating-assisted incremental forming method for CFRTP sheet – Fundamental forming characteristics in spot-forming. Procedia Engineering, **207**, 813–818 (2017). https://doi.org/10.1016/j.proeng.2017.10.834

[45] Zhang J., Taylor T., Yanagimoto J.: Mechanical properties and cold and warm forming characteristics of sandwich sheets with a three-dimensional CFRTP core. Composite Structures, **269**, 114048 (2021). https://doi.org/10.1016/j.compstruct.2021.114048

[46] Tanaka C. B., Ershad F., Ellakwa A., Kruzic J. J.: Fiber reinforcement of a resin modified glass ionomer cement. Dental Materials, **36**, 1516–1523 (2020). https://doi.org/10.1016/j.dental.2020.09.003

[47] Sundaresan V. B., Morgan A., Castellucci M.: Self-healing of ionomeric polymers with carbon fibers from medium-velocity impact and resistive heating. Smart Materials Research, **2013**, 271546 (2013). https://doi.org/10.1155/2013/271546

[48] Sessini V., Galisteo A. J. L., Leonés A., Ureña A., Peponi L.: Sandwich-type composites based on smart ionomeric polymer and electrospun microfibers. Frontiers in Materials, **6**, 301 (2019). https://doi.org/10.3389/fmats.2019.00301

[49] Ferry J. D.: Viscoelastic properties of polymers. Wiley, New York (1980).

[50] Nielsen L. E., Landel R. F.: Mechanical properties of polymers and composites. Marcel Dekker, New York (1975).

[51] Murayama T., Bell J. P.: Relation between the network structure and dynamic mechanical properties of a typical amine-cured epoxy polymer. Journal of Polymer Science Part A-2: Polymer Physics, **8**, 437–445 (1970). https://doi.org/10.1002/pol.1970.160080309

[52] Urbaczewski-Espuche E., Gerard J. F., Pascault J. P., Reffo G., Sautereau H.: Toughness improvement of an epoxy/anhydride matrix. Influence on processing and fatigue properties of unidirectional glass-fiber composites. Journal of Applied Polymer Science, **47**, 991–1002 (1993). https://doi.org/10.1002/app.1993.070470605

[53] Poonpipat Y., Leelachai K., Pearson R. A., Dittanet P.: Fracture behavior of silica nanoparticles reinforced rubber/epoxy composite. Journal of Reinforced Plastics and Composites, **36**, 1156–1167 (2017). https://doi.org/10.1177/0731684417709952

[54] Guinier A., Fournet G.: Small-angle scattering of X-rays. Wiley, New York (1955).

[55] Ke Q., Huang X., Wei P., Wang G., Jiang P.: Effect of ethylene ionomers on the properties of crosslinked polyethylene. Journal of Applied Polymer Science, **103**, 3483–3490 (2007). https://doi.org/10.1002/app.24467

[56] Gao Y., Choudhury N. R., Dutta N. K.: Effects of neutralization on the structure and properties of an ionomer. Journal of Applied Polymer Science, **124**, 2908–2918 (2012). https://doi.org/10.1002/app.35310

[57] Han K., Williams H. L.: Ionomers: Two formation mechanisms and models. Journal of Applied Polymer Science, **42**, 1845–1859 (1991). https://doi.org/10.1002/app.1991.070420706

[58] Kishi H., Naitou T., Matsuda S., Murakami A., Muraji Y., Nakagawa Y.: Mechanical properties and inhomogeneous nanostructures of dicyandiamide-cured epoxy resins. Journal of Polymer Science, Part B, **45**, 1425–1434 (2007). https://doi.org/10.1002/polb.21170

[59] Hara M., Jar P., Sauer J. A.: Dynamic mechanical properties of sulphonated polystyrene ionomers. Polymer, **32**, 1622–1626 (1991). https://doi.org/10.1016/0032-3861(91)90397-2

[60] Macknight W. J., Taggart W. P., Stein R. S.: A model for the structure of ionomers. Journal of Polymer Science: Polymer Symposia, **45**, 113–128 (1974). https://doi.org/10.1002/polc.5070450110

[61] Johnston N. J.: Synthesis and toughness properties of resins and composites. in 'Proceedings of ACEE Composite Structures Technology Conference, Seattle, USA' 75–95 (1984).

[62] Takahagi T., Ishitani A.: XPS studies by use of the digital difference spectrum technique of functional groups on the surface of carbon fiber. Carbon, **22**, 43–46 (1984). https://doi.org/10.1016/0008-6223(84)90131-3

[63] Ishitani A.: Application of X-ray photoelectron spectroscopy to surface analysis of carbon fiber. Carbon, **19**, 269–275 (1981). https://doi.org/10.1016/0008-6223(81)90072-5

[64] Nakayama Y., Soeda F., Ishitani A.: XPS study of the carbon fiber matrix interface. Carbon, **28**, 21–26 (1990). https://doi.org/10.1016/0008-6223(90)90088-G